

Electron spin coherence exceeding seconds in high-purity silicon

Alexei M. Tyryshkin¹, Shinichi Tojo², John J. L. Morton³, Helge Riemann⁴, Nikolai V. Abrosimov⁴, Peter Becker⁵, Hans-Joachim Pohl⁶, Thomas Schenkel⁷, Michael L. W. Thewalt⁸, Kohei M. Itoh² and S. A. Lyon^{1*}

Silicon is one of the most promising semiconductor materials for spin-based information processing devices^{1,2}. Its advanced fabrication technology facilitates the transition from individual devices to large-scale processors, and the availability of a ²⁸Si form with no magnetic nuclei overcomes a primary source of spin decoherence in many other materials^{3,4}. Nevertheless, the coherence lifetimes of electron spins in the solid state have typically remained several orders of magnitude lower than that achieved in isolated high-vacuum systems such as trapped ions⁵. Here we examine electron spin coherence of donors in pure ²⁸Si material (residual ²⁹Si concentration <50 ppm) with donor densities of 10¹⁴–10¹⁵ cm⁻³. We elucidate three mechanisms for spin decoherence, active at different temperatures, and extract a coherence lifetime T_2 up to 2 s. In this regime, we find the electron spin is sensitive to interactions with other donor electron spins separated by ~200 nm. A magnetic field gradient suppresses such interactions, producing an extrapolated electron spin T_2 of 10 s at 1.8 K. These coherence lifetimes are without peer in the solid state and comparable to high-vacuum qubits, making electron spins of donors in silicon ideal components of quantum computers^{2,6}, or quantum memories for systems such as superconducting qubits^{7–9}.

Silicon has been recognized as a promising host material for spin-based electronic devices where information is stored and manipulated using the spin of the electrons, rather than their charge, as in conventional electronics^{1,6,10}. It is important to distinguish between two forms of information storage within spin: first, the storage of classical information is possible using the orientation of the spin with respect to some externally applied or internal magnetic field (that is, the ‘spin-up’ or ‘spin-down’ states). This forms the basis of spintronics, and corruption of the classical information can be characterized by the longitudinal electron spin relaxation time T_1 . The electron spin is also capable of representing quantum information, using superposition states of spin-up and spin-down states with well-defined phase. This information is much richer than classical information, but often much more fragile as it requires the preservation of the full coherent spin state. The corruption of this phase information is characterized by the coherence lifetime T_2 , which, although bounded by the relaxation time T_1 , is often much lower owing to additional mechanisms which only affect the spin coherence.

Very long T_1 values have been reported for electrons bound to shallow donors in silicon. For example, T_1 for phosphorus donors approaches an hour at 1.2 K and 0.35 T and shows a strong temperature dependence at higher temperatures (Fig. 1). The temperature dependence of T_1 is well understood in terms of spin–phonon relaxation processes, including a one-phonon (direct) process, and two-phonon (Raman and Orbach) processes^{11,12}.

The electron spin coherence times T_2 of shallow donors have also been studied previously, yielding times in the range of hundreds of microseconds to tens of milliseconds^{13–17}. These times have

prompted interest in donor electrons as quantum bits (qubits), nevertheless, they are many orders of magnitude shorter than the limit of T_1 owing to the presence of additional decoherence mechanisms. One mechanism is related to the presence of ²⁹Si isotopes with non-zero nuclear magnetic moment (natural silicon contains about 4.7% of ²⁹Si). Dipole-driven flip-flops of ²⁹Si nuclear spin pairs (termed nuclear spin diffusion) are sensed by the donor–electron spin as random field fluctuations, thus driving decoherence of the electron spin^{18,19}. A solution to this problem is to use isotopically enriched ²⁸Si with a reduced abundance of ²⁹Si (ref. 13). Here, we use very high purity ²⁸Si crystals with only 50 ppm residual ²⁹Si, available through the Avogadro project²⁰. At 50 ppm ²⁹Si the nuclear spin diffusion processes are largely suppressed (on a timescale shorter than 1 s)^{18,19} and, therefore, other T_2 processes become apparent.

Measurements of T_2 using 50 ppm ²⁹Si material with a P donor density of 10¹⁴ cm⁻³ are shown in Fig. 1 (red circles), measured using a standard Hahn echo sequence (90°– τ –180°– τ –echo). For comparison, earlier measurements using 800 ppm ²⁹Si material with higher donor densities (10¹⁵–10¹⁶ cm⁻³) are also shown (blue and green circles), supporting the observation that donor electron T_2 scales inversely with the donor density. Although this data seems to show a low-temperature limit of 20 ms for the lightest doping (10¹⁴ cm⁻³), this is due to an artefact of the measurement process, known as instantaneous diffusion. This effect can be overcome (as described below), leading to longer measured T_2 times, indicated by the stars in Fig. 1. This extends the temperature range in which T_2 is bounded by T_1 , but it is clear there are other decoherence mechanisms dominating at lower temperatures, which we will

¹Department of Electrical Engineering, Princeton University, Princeton, New Jersey 08544, USA, ²School of Fundamental Science and Technology, Keio University, Yokohama, Kanagawa 2238522, Japan, ³Department of Materials, University of Oxford, Oxford OX1 3PH, UK, ⁴Institut für Kristallzüchtung, D-12489 Berlin, Germany, ⁵Physikalisch-Technische Bundesanstalt, D-38116 Braunschweig, Germany, ⁶VITCON Projectconsult GMBH, D-07745 Jena, Germany, ⁷Lawrence Berkeley National Laboratory, Berkeley, California 94720, USA, ⁸Department of Physics, Simon Fraser University, Burnaby, British Columbia V5A 1S6, Canada. *e-mail: lyon@princeton.edu.

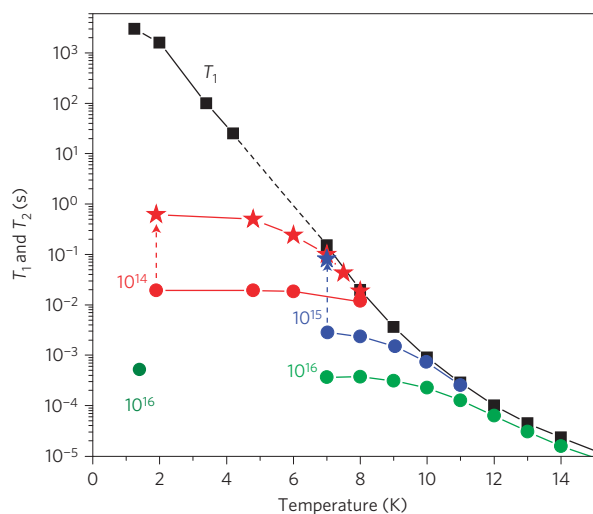


Figure 1 | Summary of measured spin relaxation times, T_1 and T_2 for phosphorus donors in silicon at cryogenic temperatures. The longitudinal spin relaxation time T_1 (squares) changes by eight orders of magnitude in the temperature range from 1.2 to 15 K, limited by one-phonon (direct) and two-phonon (Raman) relaxation processes below 4 K (ref. 11) and by an Orbach relaxation process above 7 K (refs 12,14). In contrast to T_1 , the figure shows that the transverse spin relaxation time T_2 demonstrates a substantial dependence on donor density. The T_2 data (circles marked with respective donor densities) were taken from the current work, as well as refs 13,14. T_2 is bounded by T_1 at high temperatures but then saturates at low temperatures at a level inversely proportional to donor density owing to dipolar interaction between donors (instantaneous diffusion). By suppressing instantaneous diffusion the longer (intrinsic) T_2 can be revealed (stars), limited by T_1 processes at 8 K and above, and by dipolar interactions with neighbouring donors below 8 K. The longest $T_2 = 0.6$ s measured is still more than three orders of magnitude shorter than its fundamental limit, $T_1 \sim 2,000$ s at 1.8 K.

demonstrate are related to dipolar interactions between the central donor electron and spins of neighbouring donor electrons.

Instantaneous diffusion describes decoherence of observed spins caused by flips of other dipole-coupled electron spins in the bath, as a result of the applied microwave pulses. This is clearly manifested in a dependence of the measured T_2 on the rotation angles of the microwave pulses in a Hahn echo experiment, as the effect is suppressed by using small rotation angle pulses in the refocusing pulse^{14,21,22}. Figure 2 shows two-pulse echo decays measured at 2.1 K using a ^{28}Si crystal with a phosphorus density of $1.2 \times 10^{14} \text{ cm}^{-3}$. In a standard Hahn echo experiment (Fig. 2a) with a 180° rotation angle of the second pulse ($\theta_2 = 180^\circ$), the decay is purely exponential (no spectral diffusion from ^{29}Si nuclei) and determined by instantaneous diffusion, giving a T_2 of 20 ms. On the other hand, when using $\theta_2 = 14^\circ$ for the refocusing pulse (Fig. 2b), the instantaneous diffusion is mostly suppressed and the echo decay is longer, with $T_2 = 0.45$ s.

Completely removing instantaneous diffusion would require using infinitely small rotation angles, θ_2 . However, that is not possible because the echo signal intensity also scales to zero as θ_2 decreases. An alternative approach is demonstrated in Fig. 3a, where we plot the measured $1/T_2$ as a function of $\sin^2(\theta_2/2)$ and then extrapolate the observed linear dependence to $\theta_2 = 0$ (the linear dependence is expected because of the uniform distribution of donors in silicon crystals)²². The three curves shown in Fig. 3a are for three different temperatures in the range 1.8–6 K. The slopes of the linear fits are identical at all three temperatures and match the known donor density $1.2 \times 10^{14} \text{ cm}^{-3}$ in the sample. The vertical intercept (at $\theta_2 = 0$) provides an estimate of the ‘intrinsic’ T_2 that

would be observed in the absence of instantaneous diffusion effects. It is seen that the intercept decreases as temperature is lowered, corresponding to an increase in the intrinsic T_2 . We note that the linear extrapolation in Fig. 3a also removes a further decoherence mechanism, that of dipolar flip-flops between the central spin and a neighbour spin (Fig. 3f); the small θ_2 angle makes it unlikely that both spins are flipped, and so the effect of this dipolar interaction is refocused. This has been termed the direct flip-flop process²³, and we will see below how a value for the decoherence rate of this mechanism can be obtained.

The intrinsic T_2 measured for three donor densities are plotted as a function of temperature in Fig. 3b, showing a dependence both on temperature and donor density. Three temperature regions can be identified in Fig. 3b. Above 8 K, T_2 follows T_1 for all three donor densities (dashed line in Fig. 3b). The T_1 processes (Fig. 3c) dominate donor decoherence in the high-temperature range. Below 4 K, T_2 becomes independent of temperature and saturates at a level which is inversely proportional to the donor density (Supplementary Information). As we show below, T_2 in this range is determined by spectral diffusion arising from electron spin flip-flops of nearby donor pairs (Fig. 3e), which has been called the indirect flip-flop process²⁴. At intermediate temperatures (between 4 and 8 K) there seems to be a transitional behaviour between the two extremes, however, we find that a simple sum of the two rates from the high- and low-temperature processes does not provide a good description (dotted lines in Fig. 3b). Instead a third decoherence process must be involved, which we identify as spectral diffusion caused by T_1 -induced spin flips of neighbouring donors (Fig. 3d; refs 25,26). A combination of all three processes (summing their rates with no adjustable parameters) fully explains the observed temperature dependence of T_2 for the donor densities shown in Fig. 3b (solid lines).

Both spectral diffusion processes illustrated in Fig. 3d,e are related to random fluctuations of dipole fields from neighbour donor spins decohering the central spin. However the cause of the fluctuations is different in these two processes. In one case spin–lattice relaxation (T_1) leads to random flipping of neighbouring donor spins, and in the other case dipole–dipole interactions drive spin flip-flops in neighbouring donor pairs. The theory of the first process, termed T_1 -type spectral diffusion, has been developed previously^{21,25,26}, predicting a non-exponential echo decay of the form $\exp[-(2\tau/T_{\text{SD}})^2]$, with $T_{\text{SD}}^2 \sim T_1/[P]$. In the Supplementary Information we use the measured T_1 and the known donor density $[P]$ to demonstrate that the donor two-pulse echo decays measured at 4–8 K are well described by this T_1 -type spectral diffusion without adjustable parameters. However, below 4 K, where the donor spin T_1 becomes extremely long and T_1 -induced spin flips very rare, this process no longer contributes significantly to donor decoherence.

Two experimental observations suggest that electron spin flip-flopping (Fig. 3e) in neighbour pairs is the dominant decoherence process at temperatures below 4 K: (1) T_2 shows no temperature dependence, and (2) T_2 scales with the donor density. Flip-flopping is driven by dipolar interactions and requires that the interactions be greater than the difference in resonance frequencies ($\Delta\nu = \nu_1 - \nu_2$) of the two spins involved^{3,27}. For donor densities 1.2×10^{14} – $3.3 \times 10^{15} \text{ cm}^{-3}$, as in our samples, the average donor separation is 85–250 nm, and therefore an average spin flip-flopping rate in donor pairs is about 2–40 Hz. The importance of inhomogeneous fields and their role in suppressing donor spin flip-flopping has been recently discussed by Witzel and colleagues²⁴. Assuming a donor density of $1.2 \times 10^{14} \text{ cm}^{-3}$, as in one of our ^{28}Si samples, and taking into account an inhomogeneous broadening from 50 ppm ^{29}Si , their estimate of the donor $T_2 \sim 1$ s is in agreement with the results in Fig. 3b. Remarkably, below about 8 K, the donor electron is sensitive to interactions between donors which are ~ 200 nm away. This has important implications for the

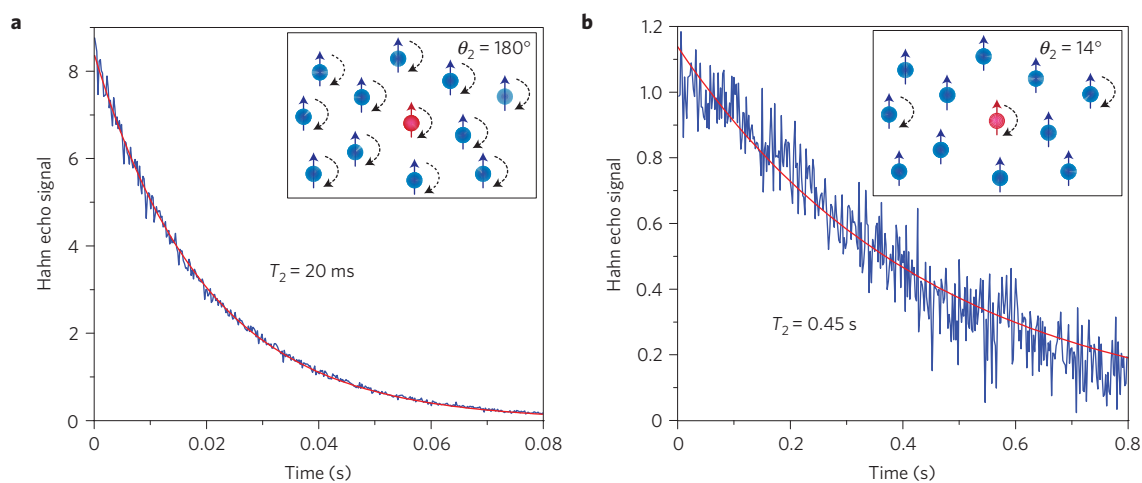


Figure 2 | Electron spin echo decays of phosphorus donors in ^{28}Si crystal with 50 ppm ^{29}Si . The two-pulse echo sequence ($90^\circ\text{-}\tau\text{-}\theta_2\text{-}\tau\text{-echo}$) was used in both cases, with the rotation angle of the second pulse set to **a**, $\theta_2 = 180^\circ$ and **b**, $\theta_2 = 14^\circ$. The relaxation decay is short in **a**, with $T_2 = 20$ ms being totally determined by instantaneous diffusion. When using a small $\theta_2 = 14^\circ$ (**b**), instantaneous diffusion is mostly suppressed, revealing a much longer $T_2 = 0.45$ s. Red curves are exponential fits. Donor concentration was $1.2 \times 10^{14} \text{ cm}^{-3}$, and temperature 2.1 K. Magnitude detection of the echo signal was used to eliminate phase noise in the signal, originating from fluctuations in the applied magnetic field¹⁴. (Insets) When using $\theta_2 = 180^\circ$, all neighbour spins (blue) are flipped by the second pulse, resulting in a large net change of dipolar interactions, as seen by the central spin (red), which leads to a strong instantaneous diffusion. Only few neighbour spins are flipped when $\theta_2 = 14^\circ$, and therefore the instantaneous diffusion is strongly suppressed.

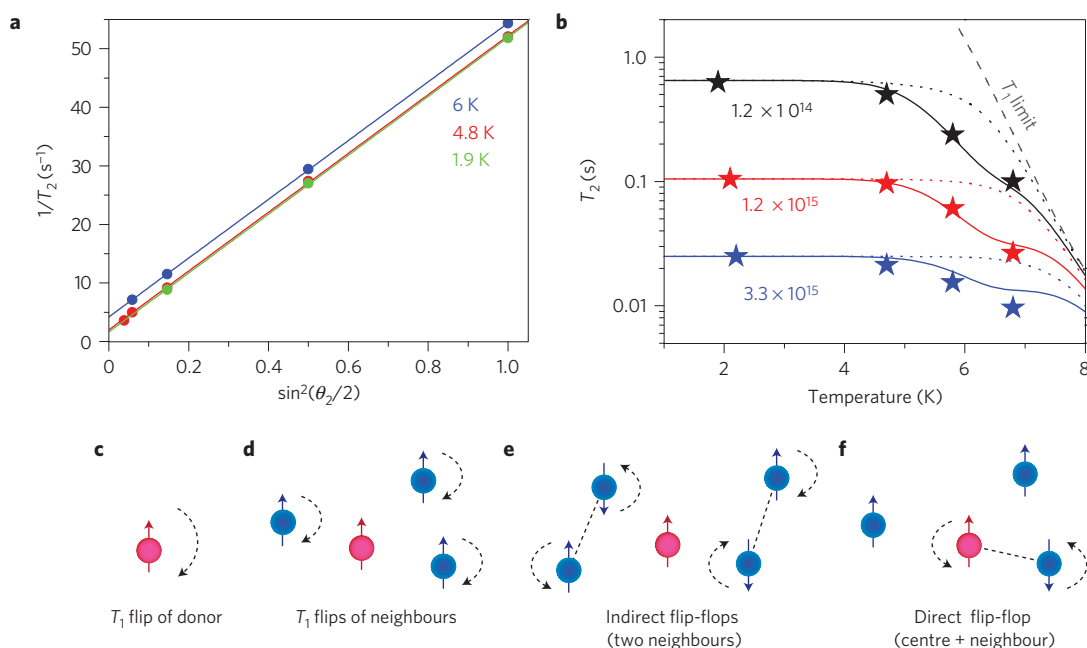


Figure 3 | 'Intrinsic' T_2 obtained by suppressing instantaneous diffusion. **a**, The experimental $1/T_2$ rates are plotted as a function of a rotation angle θ_2 , measured at three different temperatures. The slopes of the linear fits correlate with the known donor density of $1.2 \times 10^{14} \text{ cm}^{-3}$ in the ^{28}Si crystal. Intercepts obtained by extrapolating to $\theta_2 = 0$ give an 'intrinsic' T_2 corresponding to fully suppressing instantaneous diffusion. **b**, The intrinsic T_2 are plotted as a function of temperature for three ^{28}Si crystals with different donor densities as indicated. Solid lines are simulations assuming three relaxation mechanisms illustrated in **c-e**. T_1 relaxation of a central spin (**c**), T_1 -induced flips of neighbouring donor spins (**d**), and spin flip-flops in neighbouring donor pairs (**e**). Flips and flip-flops of neighbour donors (blue) produce fluctuating dipolar fields at a central spin (red) and thus dephase it. The dotted lines show a much poorer fit assuming only the two relaxation processes **c** and **e**. The dashed curve indicates the T_1 relaxation limit. Direct flip-flop (**f**) is distinct from the other processes in that the central spin is directly involved in a flip-flop event; this direct flip-flop decoheres the central spin completely.

design of donor qubit architectures and their fabrication using, for example, ion-implantation to create arrays of interacting donors. It also suggests that donor electron spins may also be useful as local spin probes at low temperature²⁸.

It is possible to control the effect of these long-range interactions and inhibit spin flip-flops by artificially increasing the offset ($\Delta\nu$) in resonant frequencies between nearby donors by applying an

external magnetic field gradient. The effect of a $10 \mu\text{T mm}^{-1}$ magnetic field gradient is shown in Fig. 4. The magnitude of the gradient was estimated from the increase in the ESR linewidth, from $3 \mu\text{T}$ to $22 \mu\text{T}$ (Fig. 4b), together with the dimensions ($2 \times 2 \times 8 \text{ mm}^3$) of our sample. The intercept after extrapolating to $\theta_2 = 0$ corresponds to an increase of the intrinsic T_2 from 1.3 ± 0.1 s in the absence of a gradient to $T_2 = 12 \pm 5$ s in the presence of the gradient.

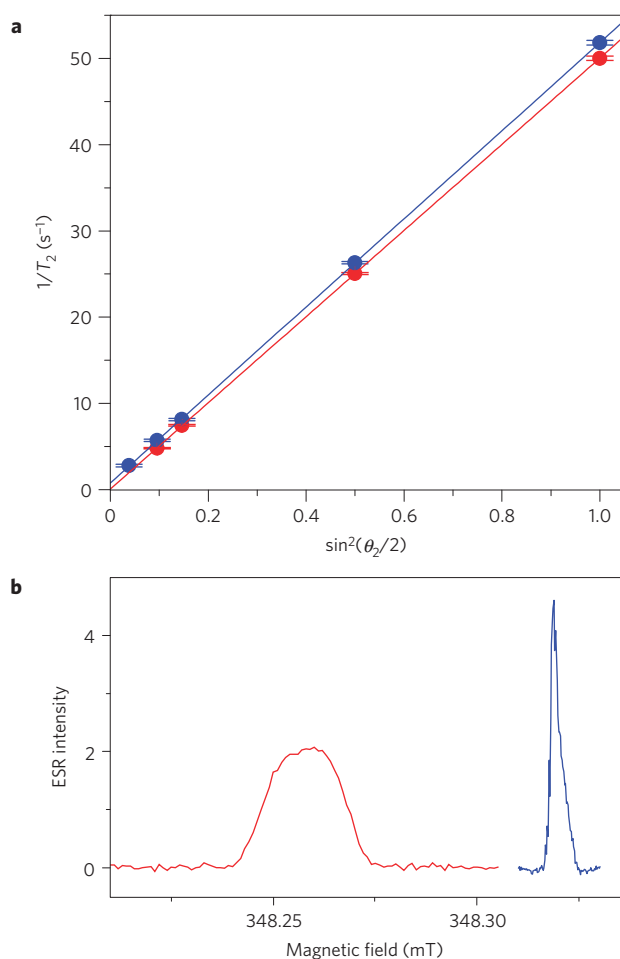


Figure 4 | Applying an external magnetic field gradient suppresses donor flip-flops and leads to an extended T_2 . **a**, The experimental $1/T_2$ rates are plotted as a function of a rotation angle θ_2 , as measured in the absence (blue dots) and presence (red dots) of an external field gradient of $10 \mu\text{T mm}^{-1}$. Error bars are well within the dots, as shown. The field gradient causes a drop in the $\theta_2 = 0$ intercept of the linear fit, such that the estimated intrinsic T_2 increases to ~ 10 s. **b** illustrates the increase of ESR linewidth from $3 \mu\text{T}$ (blue trace) to $22 \mu\text{T}$ (red trace) on applying the field gradient. Donor concentration was $1.2 \times 10^{14} \text{ cm}^{-3}$, and temperature 1.8 K.

A gradient-induced increase in the intrinsic T_2 was also observed in other ^{28}Si crystals with higher donor densities.

As seen in Fig. 4a, the slope of T_2 versus $\sin^2(\theta_2/2)$ also decreases on applying the gradient. Both changes in the intercept and the slope can be understood in terms of suppressing spin flip-flops: the intercept changes owing to suppression of the indirect flip-flops (Fig. 3e) and the slope changes owing to suppression of the direct flip-flops (Fig. 3f). Individual contributions of direct and indirect flip-flop mechanisms can be extracted from a simultaneous fit of both (gradient and no-gradient) data sets using the expression²³:

$$\frac{1}{T_2} = \sin^2(\theta_2/2) \times \left[\frac{1}{T_{2(\text{ID})}} + \frac{1}{T_{2(\text{dff})}} S_{\text{ff}} \right] + \frac{1}{T_{2(\text{iff})}} S_{\text{ff}}$$

Here we recognize that both the instantaneous diffusion ($T_{2(\text{ID})}$) and direct flip-flop ($T_{2(\text{dff})}$) processes scale as a function of $\sin^2(\theta_2/2)$, and the indirect flip-flop ($T_{2(\text{iff})}$) process is independent of θ_2 . We also introduce a flip-flop suppression factor S_{ff} (when the gradient is applied) and we assume this factor to be the same for both direct and indirect flip-flop processes. The fits, shown in Fig. 4, give $T_{2(\text{iff})} = 1.3 \pm 0.1$ s and $T_{2(\text{dff})} = 0.8 \pm 0.15$ s, whereas $S_{\text{ff}} = 13 \pm 8\%$.

The $10 \mu\text{T mm}^{-1}$ gradient introduces a shift of the resonant frequencies of $\Delta\nu \sim 100$ Hz for donors at a separation of 250 nm (corresponding to $1.2 \times 10^{14} \text{ cm}^{-3}$). Using the flip-flop suppression factor $S_{\text{ff}} = 13\%$ induced by this gradient, we then estimate the intrinsic distribution of donor resonance frequencies in the crystal to be $\Delta\nu \sim 16$ Hz before applying the gradient (see Supplementary Information). This value is a rough estimate and intended only to provide a qualitative explanation of the gradient effect. It is lower than what is expected from the random configurations of 50 ppm ^{29}Si nuclei using the Kittel–Abrahams result²⁹, which predicts $\Delta\nu \sim 280$ Hz; the discrepancy may be due to the fact that the 50 ppm abundance is far into the low-concentration limit where the Kittel–Abrahams formula loses accuracy.

To conclude, we have demonstrated that the extrapolated T_2 of electrons spins bound to donors in silicon is about 10 s at 1.8 K. This required the use of very pure ^{28}Si crystals (to reduce spectral diffusion from ^{29}Si) and the identification (and subsequent suppression) of three decoherence mechanisms arising from dipolar interactions between donor electron spins. It should be noted that the extrapolation procedure necessary to deal with the effects of instantaneous diffusion will tend to mask decoherence with a non-exponential time dependence. In particular, spectral diffusion from residual ^{29}Si has the form of an exponential of time raised to a power, and this procedure will be sensitive only to the early-time behaviour of that function, as that is when the data points are taken.

The extrapolated T_2 of ~ 10 s is still two orders of magnitude shorter than $T_1 = 2,000$ s at this temperature, and the remaining decoherence might be related to a residual donor flip-flopping that was not fully suppressed by applying the 1D field gradient, to residual ^{29}Si , or to other yet undetermined mechanisms. Further work will be required to see if T_2 can be pushed to even longer times and to identify the remaining decoherence mechanisms. Methods of further reducing the effect of donor electron spin flip-flops include using ^{28}Si with lower doping densities (but proportionally smaller signals), increasing the ratio of Zeeman energy to temperature by reducing the temperature and/or increasing the magnetic field, and refocusing the dipolar interactions with Mansfield–Rhim–Elleman–Vaughan (MREV)-type pulse sequences³⁰. For donors implanted close to a surface, as required for spin-based electronic devices, a further decoherence can arise from electric and magnetic noise associated with the surface¹⁵. The question still remains whether similarly long T_2 can be achieved for near-surface donors as those reported here for donors in bulk silicon.

Methods

High-purity ^{28}Si -enriched single crystals with phosphorus donor densities ranging from 1.2×10^{14} to $3.3 \times 10^{15} \text{ cm}^{-3}$ and a ^{29}Si concentration of 50 ppm were obtained from a dislocation free single crystal doped using PH_3 during floating-zone growth from highly enriched polysilicon²⁰. The crystals were lightly etched to remove surface damage, and dipped in hydrofluoric acid to remove surface oxides and contaminants before measurements. Pulsed experiments were performed using an X-band (9.7 GHz) Bruker spectrometer (Elexsys 580) equipped with a low-temperature helium-flow cryostat (Oxford CF935). Typical $\pi/2$ and π pulses were 40 and 80 ns, respectively. For temperatures below 5 K (when T_1 relaxation was longer than 10 s), a light emitting diode (1,050 nm) was pulsed for 50 ms after each pulsed experiment to promote a faster thermalization of donor spins. Particular care was taken to suppress mechanical (microphonic) vibrations in the cryostat setup, and to reduce the magnetic field noise introduced through pickup in the field-controller circuitry. Remaining magnetic field noise was suppressed by averaging the echo magnitude, rather than the in-phase and quadrature components of the echo signals.

Received 27 June 2011; accepted 24 October 2011; published online 4 December 2011

References

1. Appelbaum, I., Huang, B. Q. & Monsma, D. J. Electronic measurement and control of spin transport in silicon. *Nature* **447**, 295–298 (2007).
2. Kane, B. E. A silicon-based nuclear spin quantum computer. *Nature* **393**, 133–137 (1998).

3. De Sousa, R. & Das Sarma, S. Theory of nuclear-induced spectral diffusion: Spin decoherence of phosphorus donors in Si and GaAs quantum dots. *Phys. Rev. B* **68**, 115322 (2003).
4. Bluhm, H. *et al.* Dephasing time of GaAs electron-spin qubits coupled to a nuclear bath exceeding 200 μ s. *Nature Phys.* **7**, 109–113 (2011).
5. Langer, C. *et al.* Long-lived qubit memory using atomic ions. *Phys. Rev. Lett.* **95**, 060502 (2005).
6. Ladd, T. D. *et al.* Quantum computers. *Nature* **464**, 45–53 (2010).
7. Wiesenberg, J. H. *et al.* Quantum computing with an electron spin ensemble. *Phys. Rev. Lett.* **103**, 070502 (2009).
8. Kubo, Y. *et al.* Strong coupling of a spin ensemble to a superconducting resonator. *Phys. Rev. Lett.* **105**, 140502 (2010).
9. Schuster, D. I. *et al.* High-cooperativity coupling of electron-spin ensembles to superconducting cavities. *Phys. Rev. Lett.* **105**, 140501 (2010).
10. Kane, B. E. Silicon-based quantum computation. *Forts. Phys. Prog. Phys.* **48**, 1023–1041 (2000).
11. Feher, G. & Gere, E. A. Electron spin resonance experiments on donors in silicon. 2. Electron spin relaxation effects. *Phys. Rev.* **114**, 1245–1256 (1959).
12. Castner, T. G. Orbach spin-lattice relaxation of shallow donors in silicon. *Phys. Rev.* **155**, 816–825 (1967).
13. Gordon, J. P. & Bowers, K. D. Microwave spin echoes from donor electrons in silicon. *Phys. Rev. Lett.* **1**, 368–370 (1958).
14. Tyryshkin, A. M., Lyon, S. A., Astashkin, A. V. & Raitsimring, A. M. Electron spin relaxation times of phosphorus donors in silicon. *Phys. Rev. B* **68**, 193207 (2003).
15. Schenkel, T. *et al.* Electrical activation and electron spin coherence of ultralow dose antimony implants in silicon. *Appl. Phys. Lett.* **88**, 112101 (2006).
16. George, R. E. *et al.* Electron spin coherence and electron nuclear double resonance of Bi donors in natural Si. *Phys. Rev. Lett.* **105**, 067601 (2010).
17. Morley, G. W. *et al.* The initialization and manipulation of quantum information stored in silicon by bismuth dopants. *Nature Mater.* **9**, 725–729 (2010).
18. Abe, E. *et al.* Electron spin coherence of phosphorus donors in silicon: Effect of environmental nuclei. *Phys. Rev. B* **82**, 121201 (2010).
19. Witzel, W. M., de Sousa, R. & Das Sarma, S. Quantum theory of spectral-diffusion-induced electron spin decoherence. *Phys. Rev. B* **72**, 161306 (2005).
20. Becker, P., Pohl, H. J., Riemann, H. & Abrosimov, N. Enrichment of silicon for a better kilogram. *Phys. Status Solidi A* **207**, 49–66 (2010).
21. Klauder, J. R. & Anderson, P. W. Spectral diffusion decay in spin resonance experiments. *Phys. Rev.* **125**, 912–932 (1962).
22. Salikhov, K. M., Dzuba, S. A. & Raitsimring, A. M. The theory of electron spin-echo signal decay resulting from dipole–dipole interactions between paramagnetic centers in solids. *J. Magn. Reson.* **42**, 255–276 (1981).
23. Kurshev, V. V. & Ichikawa, T. Effect of spin flip-flop on electron-spin-echo decay due to instantaneous diffusion. *J. Magn. Reson.* **96**, 563–573 (1992).
24. Witzel, W. M., Carroll, M. S., Morello, A., Cywinski, L. & Das Sarma, S. Electron spin decoherence in isotope-enriched silicon. *Phys. Rev. Lett.* **105**, 187602 (2010).
25. Mims, W. B. Phase memory in electron spin echoes lattice relaxation effects in CaWO₄: Er, Ce, Mn. *Phys. Rev.* **168**, 370–389 (1968).
26. Hu, P. & Hartmann, S. R. Theory of spectral diffusion decay using an uncorrelated-sudden-jump model. *Phys. Rev. B* **9**, 1–13 (1974).
27. Zhidomirov, G. M. & Salikhov, K. M. Contribution to theory of spectral diffusion in magnetically diluted solids. *Sov. Phys. JETP USSR* **29**, 1037–1040 (1969).
28. Maze, J. R. *et al.* Nanoscale magnetic sensing with an individual electronic spin in diamond. *Nature* **455**, 644–647 (2008).
29. Kittel, C. & Abrahams, E. Dipolar broadening of magnetic resonance lines in magnetically diluted crystals. *Phys. Rev.* **90**, 238–239 (1953).
30. Rhim, W. K., Elleman, D. D. & Vaughan, R. W. Analysis of multiple pulse NMR in solids. *J. Chem. Phys.* **59**, 3740–3749 (1973).

Acknowledgements

We thank W. M. Witzel and A. Morello for helpful discussions. Work at Princeton was supported by the National Science Foundation (NSF) through the Princeton Materials Research Science and Engineering Center (DMR-0819860) and the National Security Agency (NSA)/Laboratory for Physical Sciences through Lawrence Berkeley National Laboratory (LBNL) (10000080295), at Keio by the Grant-in-Aid for Scientific Research and Project for Developing Innovation Systems by the Ministry of Education, Culture, Sports, Science and Technology, the FIRST Program by the Japan Society for the Promotion of Science, and the Japan Science and Technology Agency/UK Engineering and Physical Sciences Research Council (EPSRC) (EP/H025952/1), at Oxford by the EPSRC through the Centre for Advanced Electron Spin Resonance (EP/D048559/1), at LBNL by the US Department of Energy (DE-AC02-05CH11231) and the NSA (10000080295), and at Simon Fraser University by the Natural Sciences and Engineering Research Council of Canada. J.J.L.M. is supported by the Royal Society.

Author contributions

A.M.T., S.T., J.J.L.M., T.S., M.L.W.T., K.M.I. and S.A.L. conceived and designed the experiments. A.M.T., S.T. and J.J.L.M. performed the ESR experiments. A.M.T., J.J.L.M. and S.A.L. analysed the measurements. H.R., N.V.A., P.B., H-J.P., M.L.W.T. and K.M.I. prepared the ²⁸Si samples. A.M.T., J.J.L.M. and S.A.L. wrote the manuscript with input from the other co-authors.

Additional information

The authors declare no competing financial interests. Supplementary information accompanies this paper on www.nature.com/naturematerials. Reprints and permissions information is available online at <http://www.nature.com/reprints>. Correspondence and requests for materials should be addressed to S.A.L.